



UvA-DARE (Digital Academic Repository)

Morphometrics of modern and fossil Poaceae pollen from South America

Wei, C.

Publication date
2023

[Link to publication](#)

Citation for published version (APA):

Wei, C. (2023). *Morphometrics of modern and fossil Poaceae pollen from South America*. [Thesis, fully internal, Universiteit van Amsterdam].

General rights

It is not permitted to download or to forward/distribute the text or part of it without the consent of the author(s) and/or copyright holder(s), other than for strictly personal, individual use, unless the work is under an open content license (like Creative Commons).

Disclaimer/Complaints regulations

If you believe that digital publication of certain material infringes any of your rights or (privacy) interests, please let the Library know, stating your reasons. In case of a legitimate complaint, the Library will make the material inaccessible and/or remove it from the website. Please Ask the Library: <https://uba.uva.nl/en/contact>, or a letter to: Library of the University of Amsterdam, Secretariat, P.O. Box 19185, 1000 GD Amsterdam, The Netherlands. You will be contacted as soon as possible.





Caixia Wei & Limi Mao

Chapter 4

Evolution of the grass pollen morphology due to evolutionary processes and immigration since 23 Ma

Caixia Wei, Phillip E. Jardine, Limi Mao, Luke Mander, Mao Li, William D. Gosling, Carina Hoorn

This chapter is ready to submit.

Abstract

The history of grass-dominated biomes in South America extends back over 20 million years, yet the spatial and temporal development of these biomes and the underlying drivers remains unresolved. Here we quantify the micro-ornamentation of fossil and extant grass (Poaceae) pollen in South America to gain novel insights. We applied scanning electron microscopy and computational exine image analysis to quantify grass pollen morphological change through continental space and geological time. We assembled three spatial-temporal pollen groups: early and middle Miocene (western Amazon); the late Miocene to the Pleistocene (equatorial Atlantic and northern Venezuela); and extant pollen from across the grass phylogeny and a variety of ecosystems. We obtained data from a total of 1157 grass pollen grains and quantified 40 pollen surface features for each individual grain. The PCA analysis reveals that the three spatial-temporal groups occupy a unique, partially overlapping morphospace. The direction of the shift has remained consistent throughout time, and it can be characterized by a progression towards less dense ornamentation. Interestingly, the size of the morphospace occupied was found not to vary significantly. We hypothesize that changes in the exine of grass pollen since the early Miocene were driven by evolutionary processes (evolutionary drift and/or directional selection), and potentially immigration at the continental scale. These findings suggest a gradual, rather than punctuated, evolution of tropical grasses.

Keywords: Poaceae, Neogene, pollen evolution, quantitative image analysis, morphospace

1 Introduction

The grasses (Poaceae) are one of the most diverse angiosperm families on Earth, comprising close to 12,000 species (Dahlgren et al., 1984; Soreng et al., 2022). Today grassy biomes cover over a quarter of the planet's land surface, including temperate grasslands, tropical savannas, and croplands (Gibson, 2009; Blair et al., 2014), with open grasslands playing a crucial role on the evolution of grazing mammals through the Cenozoic (Prasad et al. 2005; Wilson et al. 2007; Jardine et al., 2012). Moreover, the evolution and development of anatomically modern humans (genus *Homo*) was profoundly intertwined with the emergence of the grassy savannas for over 2 million years (Strömberg and Staver, 2022), and ultimately, this led to agricultural societies emerging through the domestication of grasses (Linder et al., 2018). Today, grasses are an important crop plant and supplies humans with important building material and biofuels (Strömberg, 2011). The ecological and economic importance of grasses means that this plant group has received considerable attention in an effort to understand the mechanisms behind its evolutionary history and geographical expansion (Strömberg, 2011; Kirschner and Hoorn, 2020; Jaramillo, 2023).

Phytolith and molecular phylogenetic studies form the backbone of our knowledge about the evolutionary history of grasses. The fossil record of phytoliths (silica bodies produced by plants that are taxonomically diagnostic) suggests that the origin of grasses dates back in the Cretaceous (c. 100 million years ago (Ma), Prasad et al., 2005; Poinar et al., 2015; Wu et al., 2018). Molecular clock analyses suggests that multiple independent diversification events occurred within the grasses leading to the development of C4 photosynthesis from C3 ancestors since the Paleocene (Huang et al., 2022). However, our understanding of grass evolution is limited because grass phytoliths are not always present in the fossil record, and the molecular clock estimates are limited by a relies on extant taxa and therefore cannot evaluate the many species that went extinct over time.

Despite the high abundance of grass pollen in the sedimentary record, fossil grass pollen grains have not yet been used to reconstruct the diversification history and palaeoecology of grasses (Mander and Punyasena 2015; Hoorn et al., 2017; Jaramillo et al., 2017). This is because any morphological differences between the pollen grains of different grass taxa are difficult to observe using transmitted light microscopy, which is the traditional tool of researchers counting large numbers of fossil pollen grains in higher taxonomically resolved (Page, 1978; Bush, 2002; Beug, 2004; Halbritter et al., 2018). Being able to reconstruct changes in grass assemblage composition from the fossil record would allow us to compare the grasses with other major plant groups in the same sediment samples, and provide a potential counterpoint to phytolith and molecular records of the history grassy biomes. The fossil record of grass pollen therefore represents a potentially rich source of information on the history of grasses that is currently underexplored.

In this paper we tackle this problem by using a combination of scanning electron microscopy (SEM) and computational image analysis to investigate the micro-morphological change in grass pollen since c. 23 Ma in South America. Our study spans the early Miocene to the Pleistocene fossil pollen from the western Amazon, the Amazon submarine fan (Brazil) and the Maracaibo Basin (Venezuela), and extant pollen from across the grass phylogeny and from a variety of ecosystems across South America (Fig. 1). We use SEM to reveal morphological details on the surfaces of grass pollen grains (Andersen and Bertelsen, 1972; Page, 1978; Köhler and Lange, 1979; Mander and Punyasena, 2015), and use computational image analyses rooted in graph theory to quantify the morphological variation among these grass pollen grains (Mander et al. 2013).

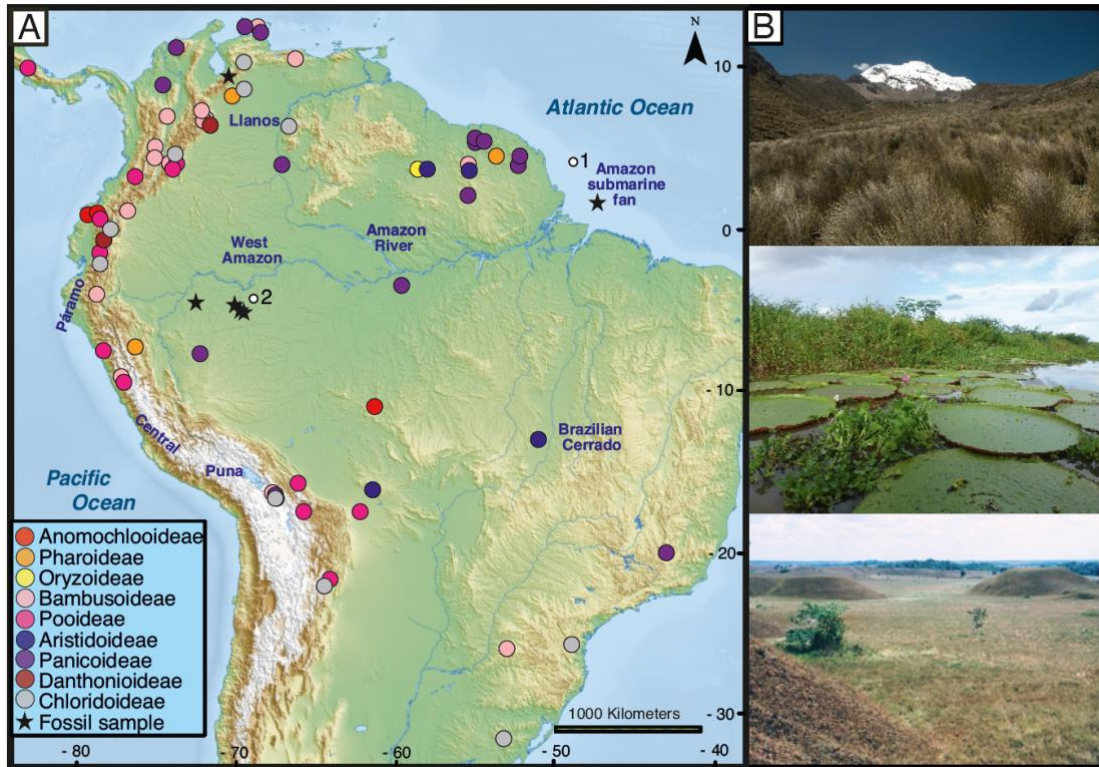


Fig. 1. A. Study sites of Poaceae fossil and extant pollen. Solid circles represent the collection localities for the extant herbarium specimens and inner circle colors denote the different grass subfamilies; black pentagrams showed the locations of fossil samples. Hollow circles symbolize the sample location of the grass pollen diagram from the literature (Hoorn et al., 2017; Kirschner and Hoorn, 2020; Jaramillo et al., 2017) shown in B. The base map was downloaded from <https://mapswire.com>. B. Different grasses habitats in present South America, from top to bottom: paramo grassland near the Chimborazo volcano in Ecuador (image credits: Esteban Suarez); grasses of the várzea near Manaus, Brazil (image credits: Carina Hoorn); savannas terrestrial of Llanos Orientales, Colombia (image credits: Henry Hooghiemstra).

Our microscale observations of pollen morphology are aimed at characterizing differences between grass pollen grains by quantifying the pollen morphological space (morphospace). We use these data to shed light on the developmental history of grass pollen, and the likely underlying mechanism driving change in our study region. We envision four potential scenarios for the expansion of the grass pollen morphospace over time in South America:

Chapter 4

In Scenario 1, we envision a shift in the extent of morphospace occupation over time. Here, we anticipate a gradual expansion of the morphospace as time passes. This pattern could be explained by the evolution, or immigration, of taxa with different pollen morphology. If this hypothesis is supported, it is expected that the morphospace of extant pollen will encompass the entire range of the fossil morphospace (Fig. 2A).

In Scenario 2, we foresee a shift in the location of morphospace occupation over time, but little change in the extent of the morphospace occupied. In this model we propose that there has either been an evolutionary drift leading to a gradual change in morphology, or balanced directional selection (extinction vs. evolution) /immigration (Fig. 2B).

In Scenario 3, we anticipate a shift in both the extent and location of the morphospace occupation. In this model we propose that directional selection, extinction, or immigration contributes strongly to changes in pollen morphology. For instance, a pulse of evolution, or a wave of new taxa arriving, into the area would result in a large expansion and change in position of the morphospace occupancy, i.e. due to geological events and/or climate change (Fig. 2C).

In Scenario 4, we anticipate no expansion in either the extent, or location, of the morphospace occupation. The morphospace occupancy of grass pollen remains highly conserved over time (Fig. 2D).

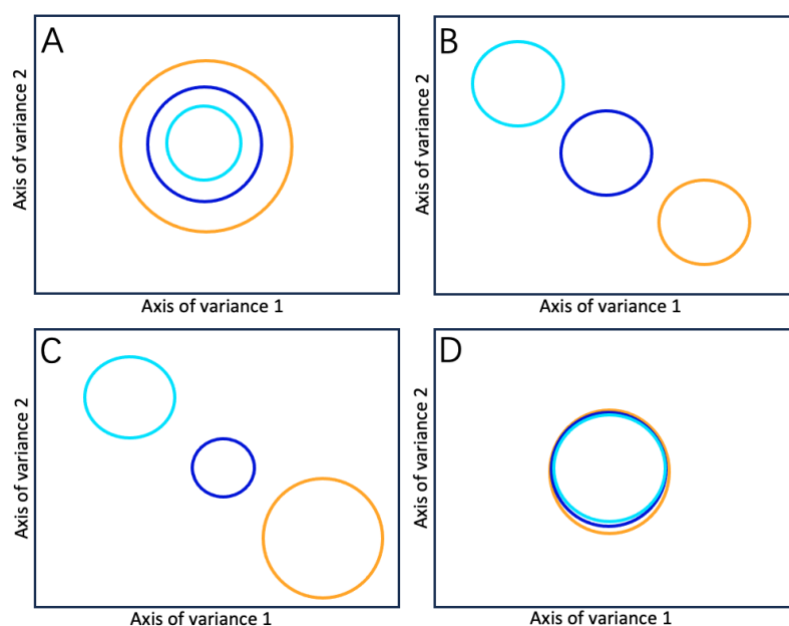


Fig 2. Possible scenarios on morphospace change for grass pollen through time. Each colored circle (cyan, blue and orange) represents the extent and location of morphospace occupancy in multi-dimensional space for a distinct time period. Scenario 1 expansion of morphospace occupation through time (A). Scenario 2 change in morphospace location (but not extent) through time (B). Scenario 3 change in morphospace extent and location through time (C). Scenario 4 morphospace stability through time (D).

2 Geological setting

Neogene uplift of the Andes has been suggested to have played a pivotal role in the landscape evolution of South America, with significant impacts on regional climate and the evolution of biodiversity over time (Hoorn, 1993; Hoorn et al., 2010; Bicudo et al., 2019; Kirschner and Hoorn, 2020). This includes the rise and demise of the megawetlands (also known as the “Pebas system”), that were situated in the western Amazon lowlands and hosted abundant grasses, but also the expansion of high *terra firme* rainforests (c. 23–9 Ma) (Wesselingh and Salo, 2006; Hoorn et al., 2010). As the uplift of the Andes continued, the Amazon River developed, transporting sediments to the Amazon delta (c. 9–2.5 Ma) (Hoorn et al., 1995; 2017; Figueiredo et al., 2009). To understand the development of grass pollen morphology

and relationship to global climate and geological event in South America, samples were divided into three spatial-temporal groups: 1) the early to middle Miocene fossil pollen from the western Amazon; 2) the late Miocene to the Pleistocene fossil pollen from the Amazon submarine fan (Brazil) and the Maracaibo Basin (Venezuela); and 3) extant pollen across the grass phylogeny and a variety of ecosystems across South America (Fig. 1).

3 Materials and Sample Processing

3.1 Collection of Specimens

Extant specimens. The Poaceae subfamily contains 12 subfamilies at the global level (Soreng et al., 2022). We restricted our research to 68 plant specimens from nine subfamilies across phylogeny and ecosystems in northern South America. Pollen was extracted from these specimens collected from the National Herbarium of the Netherlands (Naturalis) (L) (Appendix S1). All extant sample information were available through previous research (Wei et al., 2022).

Fossil materials. A total of 19 grass fossil samples were obtained from the early Miocene to the Pleistocene in South America, including nine samples from fluviolacustrine deposits in the western Amazon, nine marine samples from the Amazon submarine fan and one from Venezuela (the Maracaibo Basin) sample. The sample age and locality information are documented in Hoorn (1994); Boonstra et al., (2015); Hoorn et al. (2017, 2019, 2022); Bermúdez et al. (2017); Jardine et al. (2021) (Appendix S2).

3.2 Pollen processing.

Extant pollen. The extant pollen grains were collected from anthers of herbarium specimens and processed with standard acetolysis methods and stored in glycerin jelly (Erdtman, 1952; Faegri et al., 1989). The pollen grains were transferred from glycerin to ethanol for SEM imaging with a gradual concentration series (70%, 96%

and 100%). The pollen processing methods were available through previous research (Wei et al., 2022; 2023).

Fossil pollen. The fossil pollen was retrieved from Neogene samples of the Amazon drainage basin. The western Amazon materials and the samples from Venezuela were treated by $\text{Na}_4\text{P}_2\text{O}_7$, heavy liquid separation (clastics) and Schultze reagent (lignite) (Hoorn 1994; Boonstra et al., 2015; Hoorn et al. (2019, 2022); Bermúdez et al. (2017); Jardine et al., 2020). The Amazon submarine fan materials were processed with HCl, $\text{Na}_4\text{P}_2\text{O}_7$, acetolysis and heavy liquid separation (Hoorn et al., 2017; Jardine et al., 2020). All fossil pollen were stored in glycerin after processing. The fossil pollen grains were transferred from glycerin to ethanol with a gradual concentration series (70%, 96% and 100%) or single grain was picked by noise hair from glycerin (Zetter, 1989; Halbritter et al., 2018) ahead of scanning electron microscopy (SEM) imaging.

3.3 Scanning Electron Microscopy (SEM) imaging

Dehydrated fossil and extant pollen grains were transferred to SEM stubs and coated with Platinum gold. We imaged pollen using SEM (TESCAN MAIA3, Czech (NIGPAS, China); Zeiss Gemini Sigma 300 FEG SEM (AMC, Amsterdam)). Nine to 24 grains were examined and imaged for each extant specimen. One to 42 grains were imaged for each fossil sample depending on the pollen richness. Each pollen grain was imaged under three amplification levels: 15,000X, 75,000X, and 150,000X. All images were saved in high resolution for morphological analysis. The extant pollen images were available through previous research (Wei et al., 2023).

3.4 Quantifying Grass Pollen Morphology

We investigate the grass evolution in South America by conducting a comparative study of pollen morphology through space and time. Specifically, our study spans the early Miocene to the Pleistocene fossil pollen and extant pollen from South America. Technically, we build on the work of Mander et al. (2013) and Wei et al. (2023), by

utilizing 40-dimensional vectors (size and density of pollen surface pattern and 38 features to quantify the complexity of the surface) to quantify the morphology of individual pollen grain. This is the first application of the proposed technique to the analysis of fossil grass pollen. Our aim is to determine if the fossil and modern grass pollen have a comparable morphology and if their morphological space (from here onwards morphospace) changes over time. To achieve this, we carried out an extensive morphological analysis of fossil and extant pollen over time (Fig. 1A), and we built a SEM image library of fossil and extant grass pollen for providing a direct comparison (refer to Data accessibility).

Quantitative analysis was conducted on $3.3 \mu\text{m}^2$ (1855 X 1855 pixel) windows, manually cropped from each 150,000X SEM image of grass pollen ornamentation. From each cropped image, 40-dimensional vectors were extracted to evaluate the size, density, and complexity of pollen surface patterns. This method was adapted from the approach used for extant pollen developed by Mander et al. (2013) and Wei et al. (2023). Contrast-limited adaptive bell-shaped histogram equalization was applied for adjusting the contrast and then five sub-images with 1000 X 1000 pixels were randomly chosen and cropped from each 1855 X 1855 image (Mander et al. 2013; Wei et al., 2023). All features were calculated as the average values extracted from these five sub-images.

For the size feature, the technique employed Sobel edge detection and connected components to identify objects within the sub-image, principal component analysis (PCA) was performed to measure the **[size]** feature (Wei et al., 2023). To calculate the density feature, we applied color quantization and selected the brightest component as the foreground followed, by morphological closing, then counted connected areas as the **[density]** of the sub-image (Wei et al., 2023). All the detailed steps of construction of features size and density were available through previous research (Fig 2. of Wei et al., 2023). To assess the complexity of pollen surface patterns, we adapted the method which used the concept of subgraph centrality (SC)

developed in Mander et al. (2013). In a previous study, SEM images were first coarsely classified into four groups based on size and density. Different groups used different methods to binarize the images: some used the top two brightest components as foreground, while others used the top three brightest components (Mander et al., 2013). However, the data used in this study has more continuous size and density features, which implies that the coarse classification is not suitable. Therefore, we extracted SC features for both methods, top two brightest components (SC2) and top three brightest components (SC3) as foreground.

For the detailed approach, we first resized the sub-image with 1000X1000 pixels down to 200X200 pixels, and then cropped the center 120X120 pixels as the input image (Fig. 3 a1, c1, e1). Then we quantized each image into four colors (Fig. 3 b1, d1, f1) and binarized it by using either top two brightest components as foreground (Fig. 3 a2, c2, e2) or top three brightest components as foreground (Fig. 3 b2, d2, f2). Then we further resized the image into 40x40 pixels to save computational cost and formed a network by connecting each pixel to its four neighbors. We assigned 0.01 to the edges which connect foreground and background. The rest edges are a mathematical function SC was calculated to rank the pixels (Fig. 3 a3-f3). A sequence of 19 expanding subregions of the networks was formed, starting with the pixels ranked in the top 5% and adding the next 5% until the entire pixels was covered with number of connected component records as features [**SC2_1 to SC2_19, or SC3_1 to SC3_19**]. Earlier features such as SC2_1 and SC2_2 describe the components with higher SC values which are more centered regions in the larger “chamber”. In the middle features such as SC2_7, many larger “chambers” are connected by thin bridge and some median sized “chambers” show up; later features like SC2_18 and SC2_19 exhibit almost entire region except lower SC values which are boundary pixels and smaller “chambers”. All the detailed steps of construction of features by using the subgraph centrality (SC) were shown in Fig 3.

We automatically extracted morphological measurements from each fossil and extant grain directly from the SEM images for further analysis. The values of 40 quantitative features of each individual fossil and extant pollen grain are provided in Appendix S3 and S4, respectively.

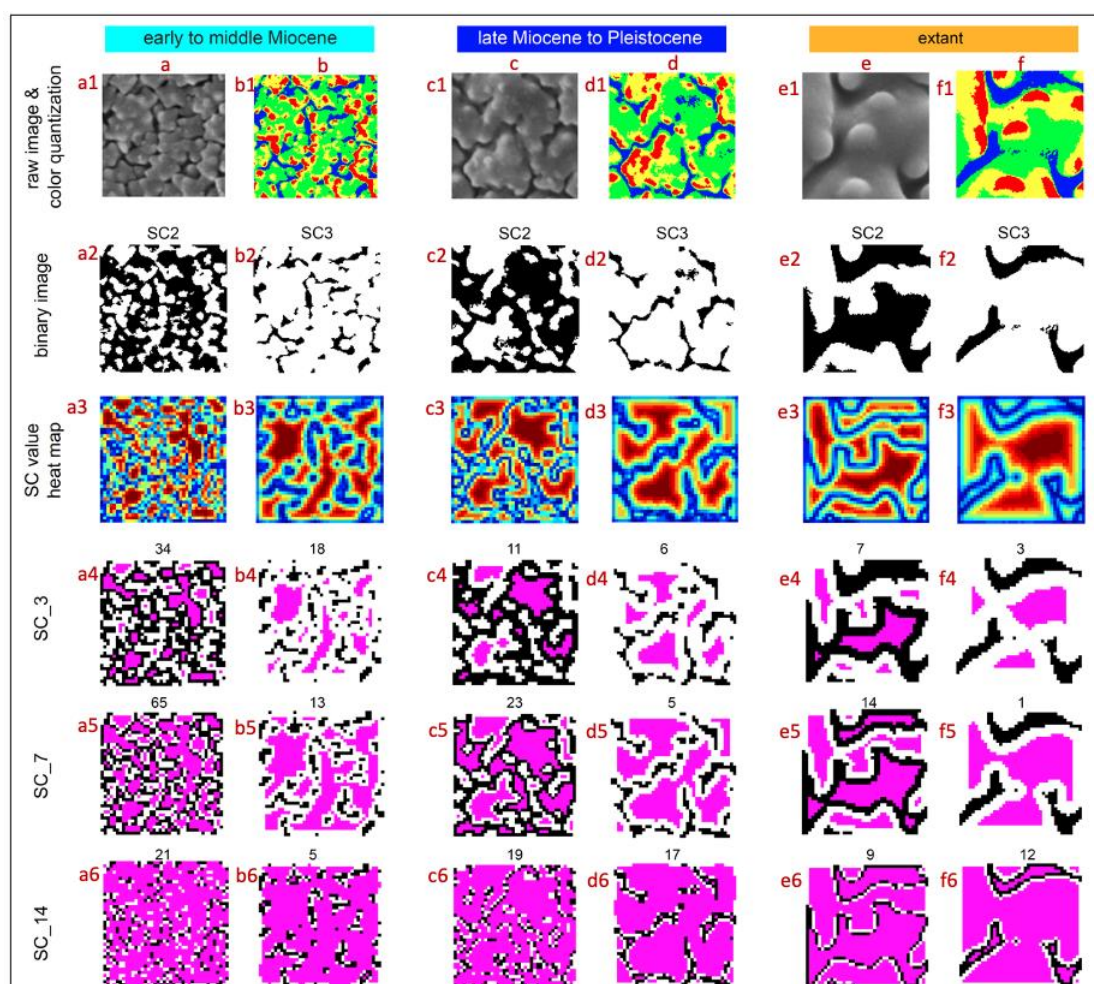


Fig. 3. Thumbnails showing the example of image processing steps that were taken during the construction of SC2 features (a, c, e) and SC3 features (b, d, f). Example grass pollen from the early to middle Miocene (a-b, from Los Chorros), the late Miocene to the Pleistocene grass pollen (c-d, from the Amazon submarine fan), and extant (e-f, *Bothriochloa saccharoides* (Sw.) Rydb.). (a1-f1) showing the raw randomly cropped sub-images (a1, c1, e1) and four colors quantization of raw images with brightness ordered from red to blue (b1, d1, f1). (a2-f2) showing two different binary images with the foreground in white, detailing in SC2 groups (a2, c2,

e2) using the top 2 brightest colors (red and yellow) and SC3 groups (b2, d2, f2) using the top 3 brightest colors (red, yellow, and green) as foreground for calculating SC2 and SC3 features, respectively. (a3-f3) showing the heatmap of subgraph centrality values (SC) with the largest value in red. (a4-f4, a5-f5, a6-f6) showing the top 15% (SC_3), top 35% (SC_7), and top 70% (SC_14) pixels by ranking the SC values and are highlighted in pink respectively, and the number above each image represents the number of connected components of the pink region which are the corresponding SC2 and SC3 feature values.

3.5 Morphometric Analysis

Comparison of Fossil and Extant Grass Pollen. The quantified features of size and density values were logged before being used in data analyses, which aimed to make the data closer to a normal distribution. We utilized scatter plots of log size and log density for basic data visualization and exploration. Further principal component analysis (PCA) of 40 quantified features (log size, log density, 19-dimensional features of SC2, and 19-dimensional features of SC3) was applied to compare the morphospace of the fossil (spatial-temporal groups 1-2) and extant pollen (group 3). The confidence ellipsoids were used to show the vector range of the PC1 and PC2 of fossil and extant pollen groups.

Exploration the Grass Development through Space and Time. PCA was employed on all 40 quantified features to compare the morphospace of pollen from three spatial-temporal groups. The confidence ellipsoids show the vector range of the PC1 and PC2, and the ellipsoids distance was calculated by using means based on 40 features.

3.6 Software

All image processing and feature extraction were carried out in MATLAB (R2017a). All data analysis and visualization were carried out using R v.4.1.1 (R Core Team, 2021).

4 Results

The Fossil and Extant Pollen Database. We produced high-resolution exine images of 1157 grass pollen grains of South America by using scanning electron microscopy, including 199 fossil grains of the western Amazon from the early to middle Miocene (the pollen count data from the samples are documented in Hoorn, 1994); 155 fossil grains from the Amazon submarine fan and the Maracaibo Basin in Venezuela, ranging in age from the late Miocene to the Pleistocene (up to c. 0.04 Ma) (the pollen count data from the samples are documented in Hoorn et al., 2017; Bermudez et al., 2017); 803 extant pollen grains representing species from across grass phylogeny and ecosystems (the SEM images from the extant samples are documented in Wei et al. (2023) (Fig. 4).

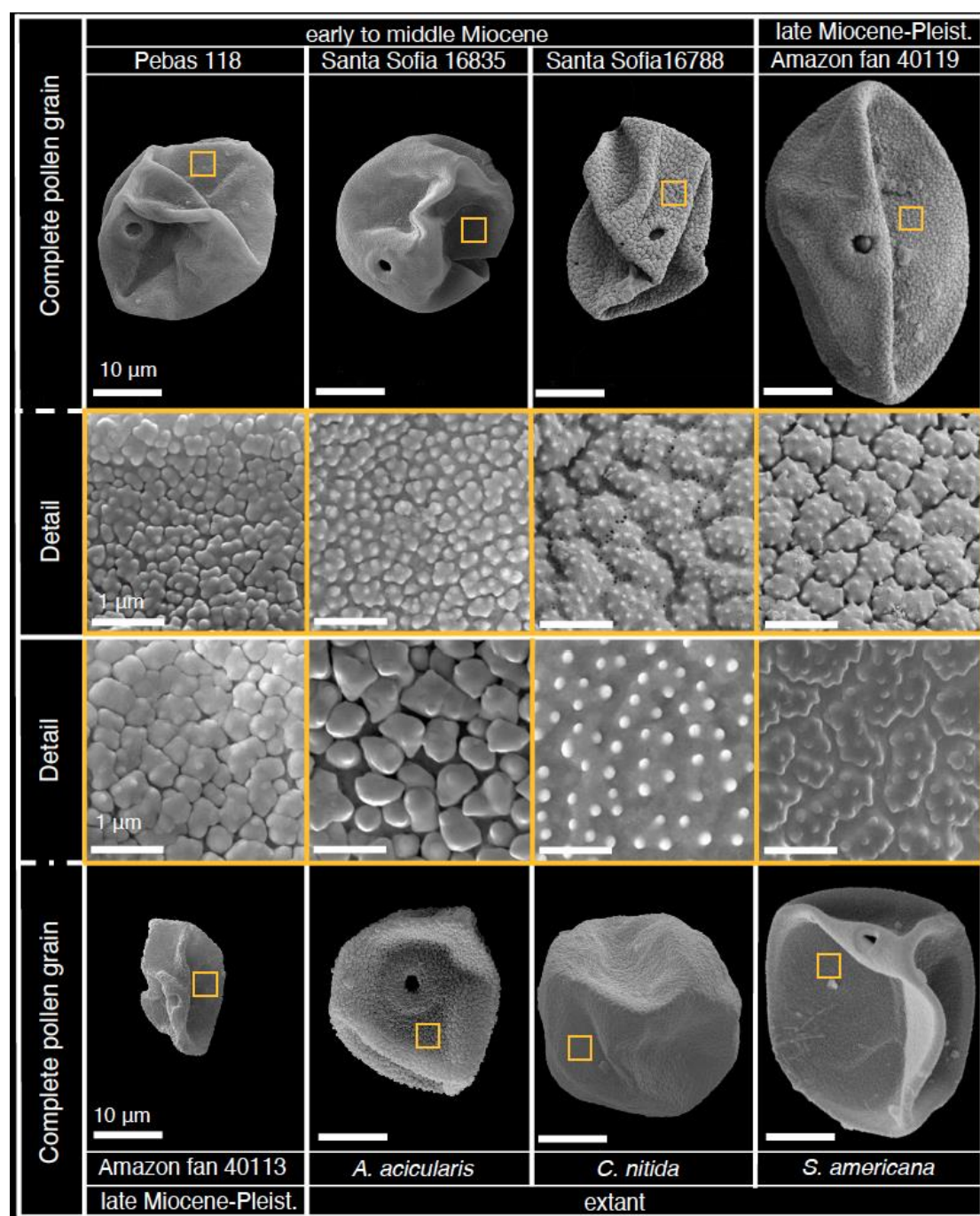


Fig. 4. Representative specimens of Poaceae pollen grains from the early Miocene to the Present. Group 1: fossil pollen of the early to middle Miocene from the western Amazon (Pebas and Santa Sofia sites; group 2: fossil pollen of the late Miocene to the Pleistocene from the Amazon submarine fan; group 3: extant pollen (*Aciachne acicularis* Laegaard., *Cortaderia nitida* (Kunth) Pilg., and *Streptogyna americana* C.E.Hubb.) from South America. The upper and bottom panels illustrate the complete pollen grains (bar = 10 μ m), the middle two panels show a surface segment. The

precise location is marked by the orange box shown in the upper and bottom panels (bar = 1 μm). All images were taken under scanning electron microscopy.

Comparison of Fossil and Extant Amazon Grasses. The quantitative measurements extracted from each individual fossil and extant pollen grain were used to construct morphospaces (Fig. 5). The preliminary exploration was conducted using a scatterplot of log size and log density of pollen surface elements, as well as confidence ellipsoids of fossil and extant groups (Fig. 5A). The scatter plot along with confidence ellipsoids show the distinct morphospace occupancy for fossil and extant grass pollen, while the position of confidence ellipsoids indicates that the values of log density in the fossil is higher than in the extant pollen. Our results suggests that the log density of grass pollen surface elements has gradually decreased over the evolutionary and time.

The PCA of all 40 quantitative features (size, density, 19 SC2 features, and 19 SC3 features), along with confidence ellipsoids of PC1 and PC2, further confirms the distinct morphometric differences between fossil and extant pollen grains (Fig. 5B). PC1 and PC2 account for 35.91% and 21.07% of the total variation in all samples, respectively. The PC1 loading shows the log density and the first 12 SC2 features (SC2_1 to SC2_12) contribute most, while first 13 SC3 features (SC3_1 to SC3_13) are main contributing to PC2. The early and middle numbers in the SC series features suggesting the difference are dominated by the larger, thicker components, and later numbers representing with detailed or thin regions (refer to Quantifying grass pollen morphology). The position of the confidence ellipsoids indicates that the values of PC1 (dominated by earlier SC2 features) has gradually decreased, suggesting the “pollen ornamentation” (i.e. areoles, spinules) are gradually enlarged through time.

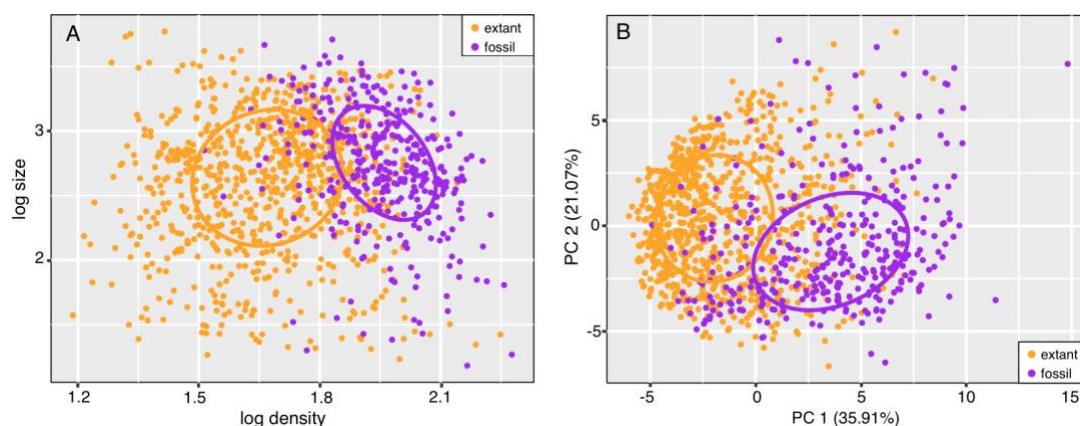


Fig. 5. A comparison of the morphospace of grass pollen micro-ornamentation between fossil samples (Miocene–Pleistocene) and extant samples from South America. A. Scatter plot and confidence ellipses of fossil and extant grass based on log size and log density. B. PCA plot and confidence ellipses of fossil and extant pollen using 40 quantitative features. The colored ellipses indicate the 50% confidence ellipsoids for fossil and extant pollen.

Grass Development through Space and Time. The PCA plots and confidence ellipsoids of PC1 and PC2 based on 40 quantitative features are utilized for both the groups of fossil pollen grains and the entire database (Fig. 6). For the PCA of just fossil groups (Fig. 6A), there is a distinction of morphospace occupancy between fossil pollen from the western Amazon of early to middle Miocene age (cyan points), and fossil pollen from the Amazon submarine fan and the Maracaibo Basin in Venezuela (blue points), dated as the late Miocene to the Pleistocene. The first two axes of a PC account for 39.67% and 22.1 %, respectively. The main contributing vectors to PC1 are SC2_9 and SC2_8, while SC2_5 and SC2_4 contribute to PC2.

When taking extant pollen into account (Fig. 6B), three spatiotemporal groups occur with unique and partially overlapping morphospace occupancy. Considering the extent of morphospace expansion, even though the pollen samples were derived from three different spatial-temporal groups, their extent—referring to the size of morphospace occupancy—did not obviously change over time. Regarding the

location of morphospace expansion, the morphometric (evolutionary) direction of these three pollen groups has remained consistent through time: the pollen morphospace occupancy shifted from the early to middle Miocene interval (cyan), to the interval of the late Miocene to the Pleistocene (blue), and then to the extant interval (orange).

The details of the PCA (percentage variance accounted for by the first two axes, and the main contributing vectors) are same within Fig.5B. While calculating the distance in ordination space between the three groups, the results showed that the distance between the early to middle Miocene group and the late Miocene to the Pleistocene group is 4.57, and the distance between the late Miocene to the Pleistocene group and the extant group is 3.3. This suggests that the late Miocene to the Pleistocene group is closer to the extant group, when compared to the early to middle Miocene group.

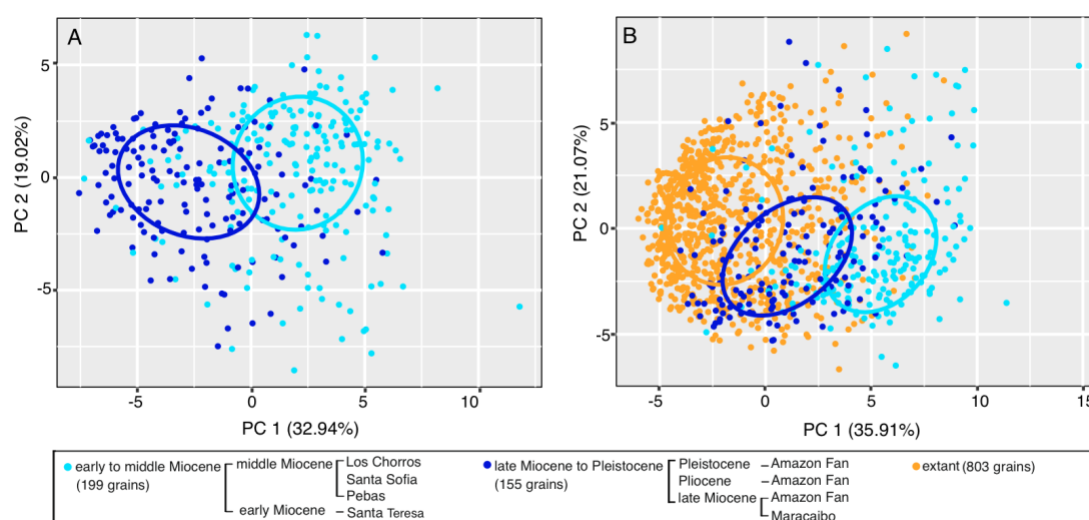


Fig. 6. The morphospace and confidence ellipsoid comparison of grass pollen micro-ornamentation through space and time. A. PCA plot and confidence ellipsoids of the range of PC1 and PC2 showing the comparison of morphospace between the two groups of fossil samples. B. PCA plot and confidence ellipsoids showing grass pollen morphospace between two groups of fossil pollen and extant pollen (note that this is

the same PCA as in Fig. 4B, but with the fossil points separated into two groups). The colored ellipse indicates the 50% confidence ellipsoids for the three pollen groups.

5 Discussion

Our study indicates that grass pollen from the early to middle Miocene interval, the late Miocene to the Pleistocene interval, and present taxa had unique but partially overlapping morphospace occupancy. The morphospace expansion of grass pollen show a change in location rather than extent through time (Fig. 6B). When considering the evolutionary rate of grass pollen in their occupancy of morphospaces over time, we observe that the distance of confidence ellipsoids from the early-middle Miocene group to the late Miocene-Pleistocene group is 4.57, while the distance to the extant group is 3.3 (Fig. 6B). The relatively small difference in distances suggests a stable speed, or modest reduction, in evolutionary rate of pollen micro-ornamentation that has been maintained over the observed time scale.

When revisiting the four scenarios we proposed earlier, our data of morphospecies occupancy were most closely aligned with Scenario 2 (Fig. 2B). This scenario suggests that a stable directional selection or drift (i.e., an evolutionary process) led to a gradual change in pollen morphology. Notably, the morphospace of the three intervals presents not distinct groups but rather unique and partially overlapping occupancies. Additionally, our study did not support the other three scenarios in terms of changes in the extent of morphospace (Fig. 2A), or in the extent and/or location of morphospace occupancy (Fig. 2C; 2D).

We anticipate that there are three possible mechanisms that can explain change in grass pollen morphology through space and time.

- a) *Chemical and /or physical alteration of the pollen wall due to post-depositional diagenetic processes.*

Sporopollenin constitutes the outer wall of both pollen and spores (Gray and Boucot, 1971; Jaramillo et al., 2006). Previous study indicated that the chemical composition of the sporopollenin can be affected by early diagenetic processes (Jardine et al., 2021). This has drawn our attention to whether pollen micro-ornamentation patterns can be influenced by chemical and/or physical alterations resulting from post-depositional processes.

In the study of Fourier transform infrared (FTIR) microspectroscopy on grass sporopollenin (Jardine et al., 2021) and the present study, fossil pollen was both taken from the Amazon submarine fan and the western Amazon (the early Miocene to the Pleistocene), and extant pollen from South America grasses. Jardine et al. (2021) suggested that fossil and extant pollen exhibited distinct groups (Fig. 7). If we envision that the pollen micro-ornamentation patterns can be affected by chemical and/or physical alteration, the diagenetic effects should lead to a clear separation between extant and fossil, as seen in the chemistry (Fig. 7), however, this is not in agreement with our pollen morphometric data (Fig. 5A; 5B).

Moreover, the grain surfaces patterns in the fossil and extant pollen showed similar and clear patterns, such as "areolae" and/or "spinules" (Fig. 3). These all suggest that micro-ornamentation, and thus physical appearance of the Poaceae pollen, is not compromised by post-depositional diagenetic processes. Our quantitative image analysis thus indicates that combining high-resolution imaging of grass pollen on both fossil and extant grains is a robust way to assess changes in the grass pollen exine, which will enable us to assess, to some degree, changes in grass biomes across space and time.

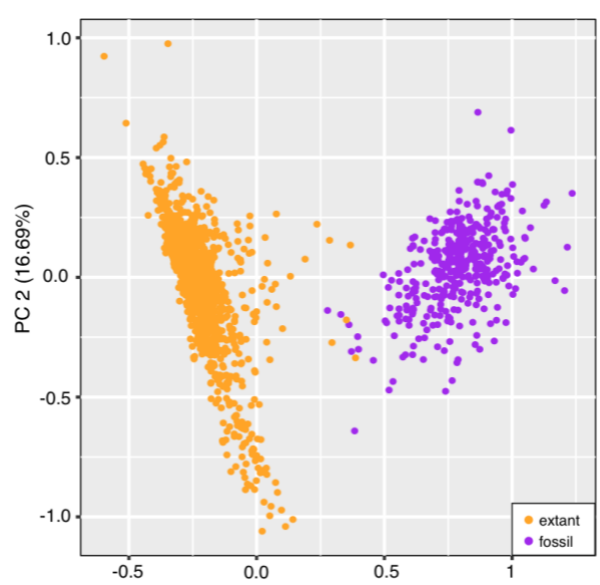


Fig. 7. Re-plotted PCA of FTIR spectra data from grass sporopollen throughout space and time (Fig 4A of Jardine et al. (2021)).

b) Are changes in the pollen wall related to abiotic turnover?

The development of grass biomes is thought to be linked to tectonism (Kohn and Fremd, 2008), climate (Edwards et al., 2010), and the combination of landscape dynamics and climate (Hoorn et al., 2023; Jaramillo, 2023). Here we question if palaeobiogeographic and palaeoenvironmental changes could have affected the grass pollen surface patterns over the time in South America. However, this scenario does not seem plausible. Recent studies on extant grass pollen morphology have demonstrated that the quantitative features (size alone or density as well as their combination) of micro-ornamentation patterns of grass pollen are not associated with climate, vegetation types, soil types, and photosynthetic pathways (Wei et al., 2023). In comparison to previous research, the extracted quantitative features of pollen micro-ornamentation were increased from two (size, density in Wei et al. (2023)) to 40 (size, density, 19 SC2 and 19 SC3). It is noteworthy that density feature still has a significant contribution in morphometric studies (Fig. 6; Fig. 7). This suggests that micro-ornamentation evolution of grass pollen is not clearly affected by abiotic factors.

We divided our grass pollen samples into three spatiotemporal groups through the Neogene in South America, that are related to a series of geological events or settings (Fig. 8). Most noticeable in this sequence is the disappearance of the megawetlands (i.e. “Pebas system”) in the western Amazon lowlands (c. 23–9 Ma) (Wesselingh and Salo, 2006; Hoorn et al., 2010). After that, the wetland transitioned into a fluvial landscape with the Amazon River having extensive flood plains (c. 9–0.5 Ma) (Hoorn et al., 1995; 2017). If we envision that the grass pollen morphology was affected by palaeogeological events and/or palaeoclimate in the certain period, we expect that some related restriction or expansion of morphospace occurred through time. (Fig. 2A). However, our results show three grass pollen groupings with unique morphospaces occupancy, their shift has remained consistent through time (Fig. 6B). This also further confirms that the micro-ornamentation morphospace of grass pollen are not driven by cross-spatiotemporal abiotic factors.

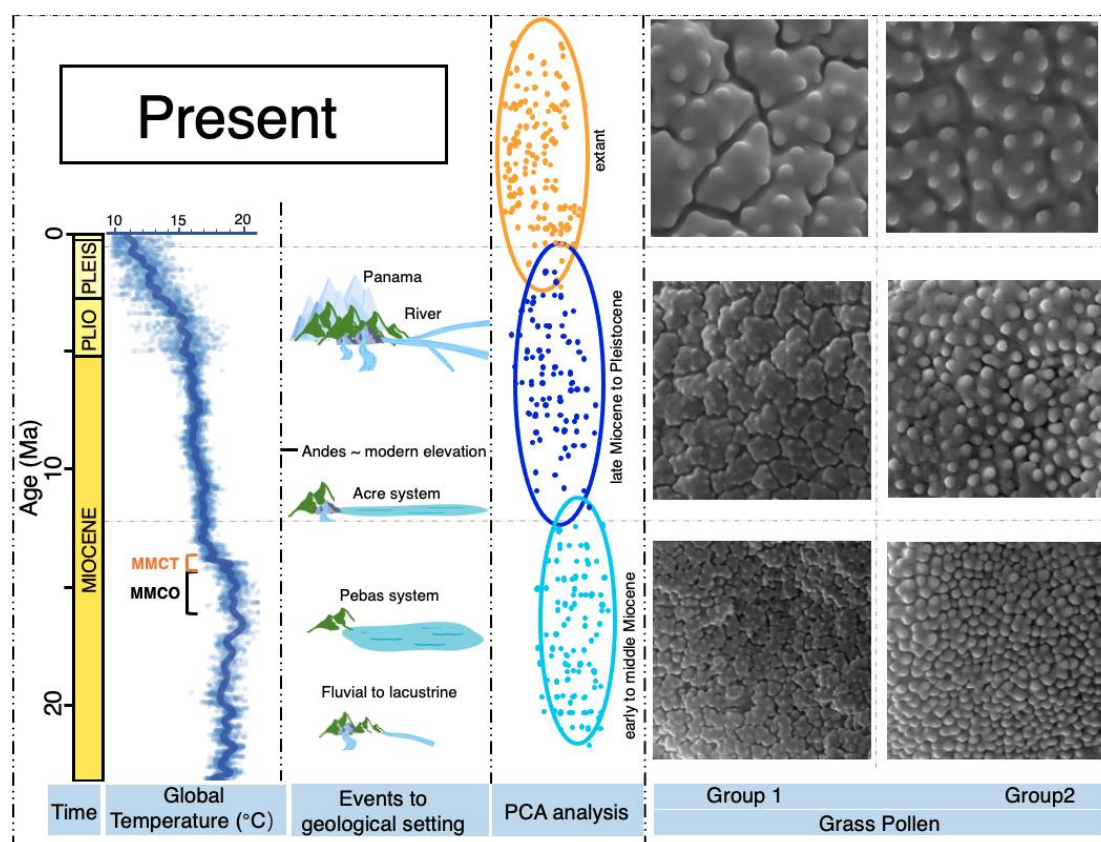


Fig. 8. Grasses development scenarios through space and time in South America. From left to right showing: the age in million years; global surface temperature curve

since Neogene (modified after Hoorn et al., 2023), MMCO (Middle Miocene Climatic Optimum, c. 16.9–14.7 Ma), MMCT (Middle Miocene Climatic Transition (MMCT), c. 14.7–13.8 Ma); overview of events to three geological setting in South America (Hoorn et al., 2010); schematic diagram illustrating the shift of pollen morphometrics from three geological setting groups over time, represented by confidence ellipses in Fig. 4B; two sets of grass pollen surface segments with similar morphology were selected from three geological setting: set 1 represents pollen surface in areolae studded with one to ten small pointed spinules (same set in Fig 2); set 2 represents single spinule or small areolae studded by one to three spinules.

c) Evolution of pollen wall morphology

Our findings demonstrate the three unique but overlapping morphospace occupancy of grass pollen shift through time. The PCA analysis indicated that the morphospace expansion of grass pollen show a change in location rather than extent through time, suggesting that pollen development towards a less dense ornamentation through time, with extinction of the denser types (Fig. 5; Fig. 6; Fig 8). We conclude that the changes in the exine of grass pollen since the early Miocene would have resulted by the directional change in pollen morphospace. We envision that the potential drivers caused the directional change in morphospace occupancy below:

c1) Evolutionary Processes

The evolutionary processes, specifically in evolutionary drift and/or directional selection, were/was expected to lead a directional development of pollen with less dense ornamentation over time.

c2) Immigration

We proposed that the shift in pollen morphology would have resulted in the appearance or extinction of new pollen morphology through the immigration of new

taxa in or old taxa out. Additionally, the extent of morphospace occupancy, in terms of the range of morphological variation, remained consistent over time.

At a global scale, diversification rates in the grass family were low during the Paleogene (c. 66–23 Ma), while increasing significantly during the Neogene (c. 23–5 Ma), which may be related to decreasing atmospheric CO₂ (Palazzesi et al., 2022). We note that within our dataset of pollen morphological changes, a gradual, rather than punctuated, development occurs for South America. These data overlap in time with the Neogene global expansion and diversification of grasses and grasslands that are highlighted by Palazzesi et al. (2022). If this morphological signal is replicated across the globe (i.e. the pattern reflects evolutionary process alone), this would suggest a decoupling of Poaceae pollen morphological evolution and global climatic change.

6 Conclusions

We conducted a broad and deep-time scale study of grass pollen to examine pollen development within the Poaceae family, and assess the underlying drivers of change since the Neogene in South America. Our study presents a novel technique for quantifying fossil pollen surface by combining SEM images of pollen ornamentation with computational image analysis. Our grass pollen morphological study reveals that the morphospace occupancy of grass pollen shows a shift in location, but not extent, over time. The shift in morphospace can be characterized as a progression towards less dense ornamentation. By exploring the underlying drivers behind the pollen morphospace expansion, we emphasize that grass pollen evolution is strongly linked to gradual directional change. We further propose that evolutionary processes (specifically in evolutionary drift and/or directional selection) and/or immigration have played roles in the evolution of grass pollen from the early Miocene to the present in South America. Our findings suggest a gradual, rather than punctuated evolution of grass pollen since c. 23 Ma.

7 Support Information

The original SEM images of modern grass pollen image can be download from previous publication: <https://doi.org/10.6084/m9.figshare.23302022.v2>

The original SEM images of fossil grass pollen image, the quantitative features extracting of pollen images, appendices, and the coding for data analysis for this study can be downloaded from: <https://figshare.com/s/111a95932f929f06db9d>